



Contents lists available at ScienceDirect

Fuel

journal homepage: www.elsevier.com/locate/fuel



Solvent free synthesis of methyl palmitate over sulfated zirconia solid acid catalyst

K. Saravanan, Beena Tyagi*, Ram S. Shukla, Hari C. Bajaj

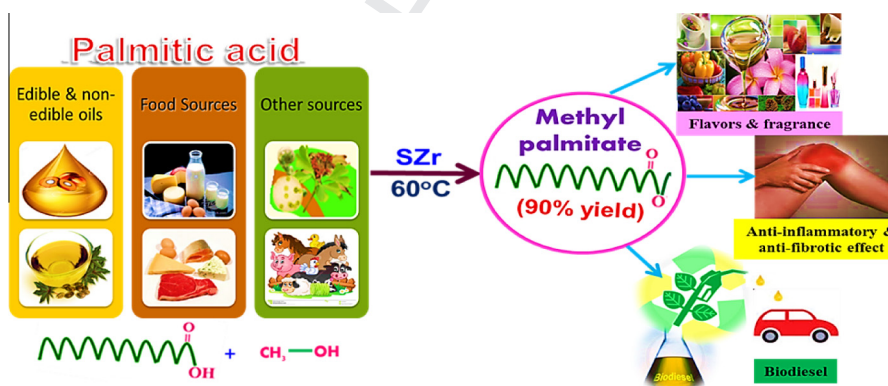
Discipline of Inorganic Materials and Catalysis, Council of Scientific and Industrial Research, Central Salt and Marine Chemicals Research Institute (CSIR-CSMCRI), G.B. Marg, Bhavnagar, Gujarat 364 002, India
Academy of Scientific and Innovative Research (AcSIR), CSIR-CSMCRI, G.B. Marg, Bhavnagar, Gujarat 364 002, India

HIGHLIGHTS

- SZr solid acid catalyst prepared by simple precipitation method and characterized.
- Excellent activity for esterification of palmitic acid with methanol.
- Higher yield of methyl palmitate under solvent free and mild reaction condition.
- Yield of alkyl palmitate decreased with methanol to *n*-butanol.
- Activity comparable with H_2SO_4 , though decreased in re-cycling due to sulfur loss.

GRAPHICAL ABSTRACT

The esterification of palmitic acid with methanol resulted into 90% yield of methyl palmitate at 60 °C over 6 wt% of conventional sulfated zirconia catalyst under solvent-free conditions.



ARTICLE INFO

Article history:
Received 19 March 2015
Received in revised form 25 July 2015
Accepted 14 October 2015
Available online xxxx

Keywords:
Esterification
Palmitic acid
Methyl palmitate
Solid acid catalyst
Sulfated zirconia

ABSTRACT

Sulfated zirconia (SZr) solid acid catalyst, prepared by conventional precipitation technique was studied for esterification of palmitic acid with methanol to synthesize methyl palmitate. The catalyst exhibited 90% yield of methyl palmitate at 60 °C over 6 wt% catalyst. The yield was significantly higher under solvent-free conditions than using hexane as a solvent. The alkyl palmitate yield was decreased with an increase in the alkyl chain of alcohol from methanol to *n*-butanol. The reaction followed pseudo-first order kinetics under the optimized reaction conditions with a reaction rate of 0.61 mmol h^{-1} , rate constant of $12.13 \times 10^{-3} \text{ h}^{-1}$ and turn over frequency of 0.088 min^{-1} .

© 2015 Published by Elsevier Ltd.

1. Introduction

The fatty acid alkyl esters are widely used in the production of fuel, cosmetics and detergents in the chemical industry. In the last decade, esterification of long chain fatty acids with short chain alcohol has spurred to the scientific community with the

* Corresponding author at: Discipline of Inorganic Materials and Catalysis, Council of Scientific and Industrial Research, Central Salt and Marine Chemicals Research Institute (CSIR-CSMCRI), G.B. Marg, Bhavnagar, Gujarat 364 002, India. Tel.: +91 278 2567760; fax: +91 278 2566970.
E-mail address: btyagi@csmcri.org (B. Tyagi).

emergence of biodiesel as a promising renewable energy source [1]. Biodiesel consists of mixture of methyl or ethyl fatty acid esters resulting either from the esterification of fatty acids using acid catalysts or the transesterification of oil with base catalysts. Though the production of biodiesel via transesterification of oils with conventional base catalysts is commercialized, the esterification of low-cost feedstock such as non-edible oils and animal fats having higher free fatty acid contents is an essential step to avoid soap formation that reduces the biodiesel yield [2]. There are four methods namely acid catalyzed esterification [3], steam injection [4], chromatography [5] and film vacuum evaporation [6] for removing free fatty acids from low-cost feedstock. Among the different possible methods, the esterification method is advantageous over the other methods as it directly yields fatty esters [1,7]. Among various saturated fatty acids, palmitic acid ($C_{16}H_{32}O_2$) is present in all edible and non-edible oils in varying amount (4–23%). It is one of the major components (48%) of palm oil among total saturated fatty acids (54%) [8] that is used to produce methyl palmitate, a significant component of biodiesel. Methyl palmitate is also used in flavors and fragrance and biologically has anti-inflammatory and anti-fibrotic effect [9].

Conventionally, homogenous acid catalysts including strong Brønsted mineral acids (e.g. sulfuric or hydrofluoric acid) and *p*-toluenesulfonic acid have been used for esterification reaction. However, these acids lead to serious contamination and corrosion problems and require neutralization before disposal of waste and purification of the product [10,11] and thus homogeneous acid-catalyzed systems are not a good choice for commercial applications [12]. Therefore the extensive demand for cleaner methodologies emerged eco-friendly heterogeneous acid catalysts that can be easily separable and re-usable.

A number of solid acid catalysts have been studied for the esterification of fatty acids [13–15], intensive efforts are still going on to search a better catalyst. The solid acid catalyst should have low cost, necessary strong acid sites, high activity and selectivity for desired product at mild reaction conditions of low acid/alcohol ratio, catalyst amount and temperature. Several reports on the esterification of palmitic acid showed that various solid acid catalysts such as WO_x loaded on ZrO_2 [16] and $ZrPO_4$ [17], sulfonated carbon and chitosan [18], silica supported heteropolyacid [19], MCM-41 [20], silica [21] or niobia [22] supported and ammonium salt [23] of 12-tungstophosphoric acid were found to have good catalytic activity; however, appreciable yields of methyl palmitate could be achieved at higher acid to methanol ratio (1:30 to 1:270) [17,18,20,22–24], reaction temperature (64–200 °C) [23,25,26] and reaction time of 24–30 h [17,21] over 10–100 wt% catalyst [21,24–27]. The undesirable by-product namely dialkyl ethers are also formed due to etherification reactions under harsh reaction conditions [28]. These stringent conditions are not favorable from economic and industrial point of view. Besides these catalysts, only few studies have been reported for esterification of palmitic acid on SZr solid acid catalyst [27,29]; however higher acid to methanol ratio (1:40) and catalyst amount (15 wt %) are reported to obtain 89–97% conversion of palmitic acid at 60–95 °C temperature. SZr incorporated in SBA-15 has also been reported to exhibit 89% conversion at 68 °C with a higher acid to methanol ratio of 1:80 [29].

Herein, we report a systematic study of esterification of palmitic acid with methanol at lower acid to methanol ratio over SZr catalyst, prepared by simple conventional method. The effects of various reaction parameters such as acid to alcohol molar ratio, catalyst amount, reaction temperature, time, stirring speed along with other short chain alcohols namely ethanol, *n*-propanol and *n*-butanol have been studied. The re-cycling of SZr catalyst and important factors leading to its deactivation during its re-cycling has also been addressed.

2. Experimental

2.1. Catalyst synthesis

SZr catalyst was prepared using a conventional precipitation technique as described previously [30a]. In a typical synthesis procedure, aqueous solution of $ZrOCl_2 \cdot 8H_2O$ (s.d.fine-chem. Ltd.) was hydrolyzed by drop-wise addition of aqueous ammonia (25%; Rankem, India) under continuous stirring until the pH became 10. The precipitates were filtered, washed with distilled water until free from chloride ions (checked by $AgNO_3$ solution). The catalyst was dried in an oven at a temperature of 110 °C for 12 h and treated with H_2SO_4 (1 N, 15 ml/g) for 30 min followed by calcination at 600 °C for 4 h.

2.2. Catalyst characterization

2.2.1. Structural, textural and morphological properties

The crystallinity and the crystalline phase of prepared SZr catalyst was determined by X-ray powder diffractometer (Philips X'pert, The Netherlands) using $Cu K\alpha$ radiation ($\lambda = 1.54059 \text{ \AA}$). The crystallite size was determined from the characteristic peak of tetragonal phase of zirconia ($2\theta = 30.3^\circ$) using Scherrer formula [31]. FT-IR spectrum of the catalyst was recorded by FT-IR spectrophotometer (Perkin Elmer, GX, USA) in the range of 400–4000 cm^{-1} with a resolution of 4 cm^{-1} as KBr pellets. The bulk sulfur (wt%) retained in calcined catalyst was analyzed by elemental analyzer (Perkin Elmer 2400, USA).

Specific surface area, pore volume and pore size distribution of the catalyst was determined from N_2 sorption isotherms at $-196^\circ C$ (ASAP 2010, Micromeritics, USA). Surface area and pore size was calculated by BET (Brunauer–Emmett–Teller) equation and BJH (Barrett–Joyner–Halenda) method, respectively. The sample was degassed under vacuum ($1 \times 10^{-3} \text{ mm Hg}$) at 120 °C for 4 h, prior to adsorption measurement to evacuate the physisorbed moisture.

The microscopic study was done by SEM and TEM micrographs that were obtained using a scanning electron microscope (Leo series VP1430, Germany) and a transmission electron microscope (Jeol JEM 2100, USA), after dispersing the catalyst sample in ethanol by sonication and deposited on an Al grid coated with gold using a Polaron Sputter Coater (for SEM) and on a Cu grid coated with carbon film (for TEM).

2.2.2. Acidic properties

The total surface acidity of the catalyst was measured by temperature programmed desorption (TPD) of NH_3 (Micromeritics Pulse Chemisorb 2720) by standard procedure as described earlier [30b].

Brønsted and Lewis acid sites were differentiated using pyridine as a probe by FT-IR spectrophotometer (Perkin Elmer, GX, USA) equipped with Diffuse Reflectance FT-IR (DRIFT) accessory (Graseby Specac, P/N 19900) and an automatic temperature controller (Graseby Specac, P/N 20130) as described earlier [32]. The quantification of B and L acid sites ratio (B/L) was done from the characteristic peak area of 1545 cm^{-1} for B and 1442 cm^{-1} for L at 150 °C as well as by molar extinction coefficient method (using $\epsilon_B = 1.67 \text{ cm}^2/\mu\text{mol}$ and $\epsilon_L = 2.22 \text{ cm}^2/\mu\text{mol}$) [33,34].

Vapor phase cyclohexanol dehydration to cyclohexene in a fixed bed reactor was used as a model reaction to assess the Brønsted acidity of the catalysts. Cyclohexanol (2 ml) was delivered by a syringe pump injector (Cole Parmer, 74900 series) with a flow rate of 1 $ml\ h^{-1}$ under N_2 at 175 °C over the catalyst sample (0.2 g) (*in situ* activated at 450 °C for 2 h) packed in a reactor bed. Product samples were collected after 1 h and analyzed with a Hewlett–Packard

gas chromatogram (HP 6890) having FID detector. The conversion of cyclohexanol and selectivity for cyclohexene was calculated by GC on weight percent basis.

2.3. Esterification of palmitic acid with methanol

Esterification of palmitic acid with methanol along with other short chain alcohols was carried out in a liquid phase batch reactor. In a typical reaction procedure, 3 mmol of palmitic acid (0.775 g, 99%, SRL Pvt. Ltd.), 60 mmol of anhydrous methanol (~1.98 g, 99.8%, SRL Pvt. Ltd.) and desired amount of the catalyst were taken in a round bottom flask and the reactant mixture was magnetically stirred at 700 rpm in an oil bath maintained at constant temperature of $60 \pm 1^\circ\text{C}$ for 7 h. The catalyst was separated from the reaction mixture by centrifugation and product was obtained after removal of methanol by rotatory evaporator. The yield of methyl palmitate (%) was analyzed by ^1H NMR in chloroform- d (99.8%, Sigma–Aldrich) solvent using following equation:

$$\text{Yield of methyl palmitate (\%)} = 100 \times (A_{\text{ME}}/3A_{\alpha\text{-CH}_2})$$

where A_{ME} = integrated area of methoxy hydrogen ($\text{CH}_3\text{O}-$) signal at 3.66 ppm and $A_{\alpha\text{-CH}_2}$ = integrated area of α -methylene hydrogen (at α position to the carbonyl group) at 2.26–2.38 ppm. The factors 2 and 3 are derived from the fact that the methylene carbon possesses two hydrogen atoms and the methyl (methanol derived) carbon has three attached hydrogen atoms [35].

The yield of other alkyl ($C = 2, 3, 4$) palmitate (%) was estimated by the following equation:

$$\text{Yield of alkyl palmitate (\%)} = 100 \times (A_{\text{CH}_2\text{-OR}}/A_{\alpha\text{-CH}_2})$$

where $A_{\text{CH}_2\text{-OR}}$ is the area of methylene protons (4.2–4.0 ppm) of the ethoxy, propoxy and butoxy group in the ester ($R = \text{C}_2\text{H}_5, \text{C}_3\text{H}_7, \text{C}_4\text{H}_9$) and $A_{\alpha\text{-CH}_2}$ is the total area of $\alpha\text{-CH}_2$ signals (2.4–2.2 ppm) of acid and ester [35].

The acid base titration with 0.1 N alcoholic KOH using phenolphthalein indicator has also been done with time to estimate the conversion of palmitic acid on the basis of acid value. For kinetic studies, aliquots were taken at desired time and concentration of palmitic acid and methyl palmitate were determined to find out the rates, v and v_1 , and rate constants, k [35].

3. Results and discussion

3.1. Characterization of SZr catalyst

3.1.1. Structural and textural properties

X-ray diffraction pattern of SZr catalyst after calcination at 600°C showed predominantly tetragonal crystalline phase ($2\theta = 30.4^\circ, 35.3^\circ, 50.2^\circ, 60.2^\circ$) (Fig. 1a) having a nano-crystallite size of 11 nm (Table 1).

FT-IR-spectrum exhibited the presence of sulfate bands at 1234, 1135, 1071, 1047 and 996 cm^{-1} (Fig. 1b), characteristic of inorganic chelating bidentate sulfate which are assigned to asymmetric and symmetric stretching frequencies of $\text{S}=\text{O}$ and $\text{S}-\text{O}$ bonds with C_{2v} symmetry and ν_3 and ν_1 stretching mode of SO_4^{2-} groups [36]. The absence of covalent $\text{S}=\text{O}$ band at $\sim 1400\text{ cm}^{-1}$ confirmed the partial ionic nature and hydrated state of sulfate groups at the surface of zirconia. A broad peak at 3363 cm^{-1} attributed to the $\nu_{\text{O}-\text{H}}$ stretching mode of water with hydrogen bonding and a peak at 1623 cm^{-1} attributed to $\delta_{\text{O}-\text{H}}$ bending mode of water molecules associated with the sulfate group and zirconia surface was observed in catalyst. The total bulk sulfur content present in the sample was 3.49 wt% that was decreased to 1.64 wt% after calcination at 600°C (Table 1).

N_2 sorption isotherm of the catalyst showed a well-defined isotherm of mesoporous materials [37] with type IV isotherm having a H2 hysteresis loop from 0.4 to 0.7 relative pressure (Fig. 2a). t-plot analysis indicated the presence of very small amount of micropores also (Table 1). BET surface area and total pore volume were $107\text{ m}^2/\text{g}$ and $0.11\text{ cm}^3/\text{g}$, respectively. The average pore diameter was 33 \AA having a narrow pore size distribution (Fig. 2b).

The surface morphology of the catalyst examined by SEM was found to have irregular rectangular-shaped particles (Fig. S1a). TEM micrograph of the catalyst showed the aggregate of irregular rectangular-shaped particles (Fig. S1b). The high-resolution TEM (HR-TEM) image (Fig. S1c) exhibited the lamellar porous structure fringes and the width between two lattice fringes (2.93 \AA) of the lamellar structure agreed with d -spacing (2.94 \AA) of characteristic peak of tetragonal (1 1 1) zirconia ($2\theta = 30.4^\circ$) shown by PXRD.

3.1.2. Acidic properties

The total surface acidity of the catalyst analyzed by NH_3 -TPD was 1.73 mmol/g (Table 1). The ammonia desorption curve of the catalyst showed the desorption peaks at 96, 545 and 799°C , which are ascribed as weak, medium and strong acid sites, respectively and were in the order of weak > strong > medium acid sites (Fig. S2).

The DRIFT spectrum of pyridine adsorbed catalyst was used to differentiate the Brønsted (B) and Lewis (L) acid sites of SZr catalyst. It exhibited the characteristic peaks for pyridinium ion (B) at 1544 cm^{-1} and covalently bonded pyridine (L) at 1443 cm^{-1} along with peak at 1490 cm^{-1} representing the combined B and L acid sites (Fig. S3). The peaks at 1614 and 1638 cm^{-1} also showed the presence of L and B acid sites respectively [38]. Brønsted acid sites were observed to be strong enough as they were present even after heating at 450°C ; though the intensity of the peaks was decreased after successive heating. However, Lewis acid sites (1443 cm^{-1}) showed only a small peak at 450°C (Fig. S3). The results indicated the presence of higher Brønsted acidity than Lewis acidity. The B/L acid site ratio was calculated by two methods; from characteristic peak area of 1541 and 1442 cm^{-1} at 150°C ($\text{B/L} = 1.39$) and molar extinction coefficient method ($\text{B/L} = 1.48$) (Table 1). B/L ratio, calculated by both methods, was in good agreement and confirmed the presence of higher Brønsted acidity in the catalyst.

The vapor phase dehydration of cyclohexanol to cyclohexene has been used as a model reaction to access the Brønsted acidity of the catalyst. The results showed 92% conversion of cyclohexanol with 100% selectivity for cyclohexene (Table 1). This further confirmed the presence of higher Brønsted acidity in the catalyst.

3.2. Esterification of palmitic acid with methanol

The effect of various reaction parameters such as palmitic acid to methanol molar ratio, reaction temperature, time, catalyst amount, stirring speed along with other short chain alcohols namely ethanol, n -propanol and n -butanol have been studied to optimize the parameters to obtain maximum yield of methyl palmitate.

3.2.1. Effect of acid to methanol ratio

The reaction was studied with an acid to methanol molar ratio in the range of 1:5 to 1:30 over 1 wt% catalyst concentration (with respect to acid) at 60°C for 7 h. At lower acid to methanol molar ratio of 1:5, the yield of methyl palmitate was 32%, which enhanced to 60% by increasing the acid to methanol ratio to 1:20 (Fig. 3a) as the excess methanol shifted the equilibrium to the product side. By further increasing the acid to methanol ratio to 1:30, the yield of methyl palmitate was decreased to 43%. The further excess of methanol than the optimum requirement may have

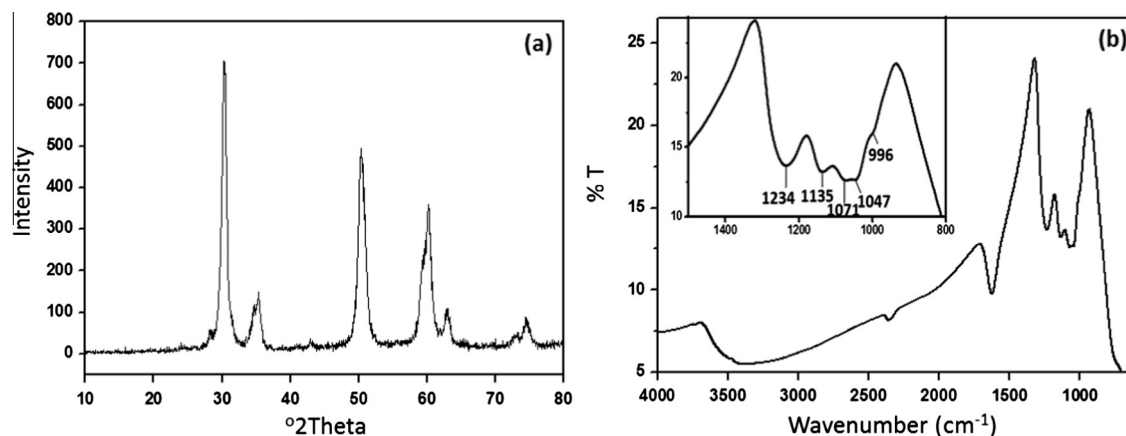


Fig. 1. (a) PXRD pattern and (b) FT-IR spectrum of SZr catalyst.

Table 1

Physico-chemical characterization of SZr catalyst.

Crystallite size (nm)	11
Sulfur (wt%)	1.64
BET surface area (m ² /g)	107
Average pore volume (cm ³ /g)	0.11
Micropore volume (cm ³ /g)	0.0013
BJH pore diameter (Å)	33
Total acid sites (mmol/g)	1.73
B/L ratio	1.39 ^a (1.48 ^b)
Cyclohexanol conversion (%)	92

^a By characteristic peak area at 150 °C.

^b By molar extinction coefficient method.

dilution effect by deluging the active sites of the catalyst that may hamper the protonation of acid at the active sites and thus resulted into lower activity. Hence, acid to methanol molar ratio 1:20 was chosen as optimal for further studies.

The yield of methyl palmitate calculated by ¹H NMR was found similar to the conversion of palmitic acid on the basis of acid value using acid base titration in presence of the catalyst. No dehydrated or etherification product of methanol was detected by GC–MS analysis under the studied reaction conditions.

3.2.2. Effect of reaction temperature

The effect of reaction temperature was studied in the temperature range of 50–60 °C over 1–3 wt% catalyst amount. The yield of methyl palmitate was increased from 49% to 60% by increasing the temperature from 50 to 60 °C over 1 wt% catalyst after 7 h (Fig. 3b).

With higher amount of 3 wt% catalyst the yield of methyl palmitate was increased from 56% to 76% over the same temperature range. As palmitic acid is insoluble in methanol at room temperature, its solubility increases with temperature and at higher temperature it homogeneously mixed well with methanol resulting into higher yield as increase in temperature facilitates the protonation of the carbonyl group of acid and favor the methanol nucleophilic attack on the acid. As boiling point of methanol is ~64 °C, the present study has been done at 60 °C.

3.2.3. Effect of alcohol chain length

Besides methanol, esterification of palmitic acid was also studied with other short chain alcohols namely ethanol, *n*-propanol and *n*-butanol. The results showed the successive decrease in the yield of ethyl palmitate to butyl palmitate (47–10%) at 60 °C (Fig. 4). By increasing the reaction temperature to reflux conditions, near to the boiling point temperature of the respective alcohol (75–115 °C), the yield of ethyl palmitate to butyl palmitate was increased (65–25%). The decrease in alkyl palmitate yield was due to the inductive effect of increased carbon chain of alcohol as the electron donating ability of alkyl group increases with increasing the alkyl chain of alcohol and thus lowers the electrophilic attack by the acid. In our previous report of esterification of myristic acid [30b], the yields of corresponding alkyl myristate were significantly increased at reflux temperature and were near to the yield of methyl myristate (98%) at 60 °C; however, the yields of corresponding alkyl palmitate in the present study were increased moderately at reflux temperature and were

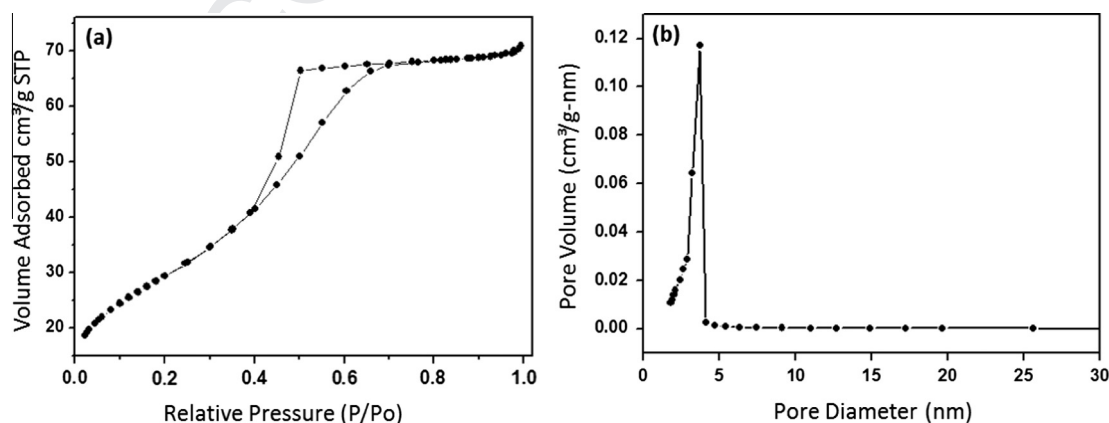


Fig. 2. (a) Nitrogen sorption isotherm and (b) pore size distribution profiles of SZr catalyst.

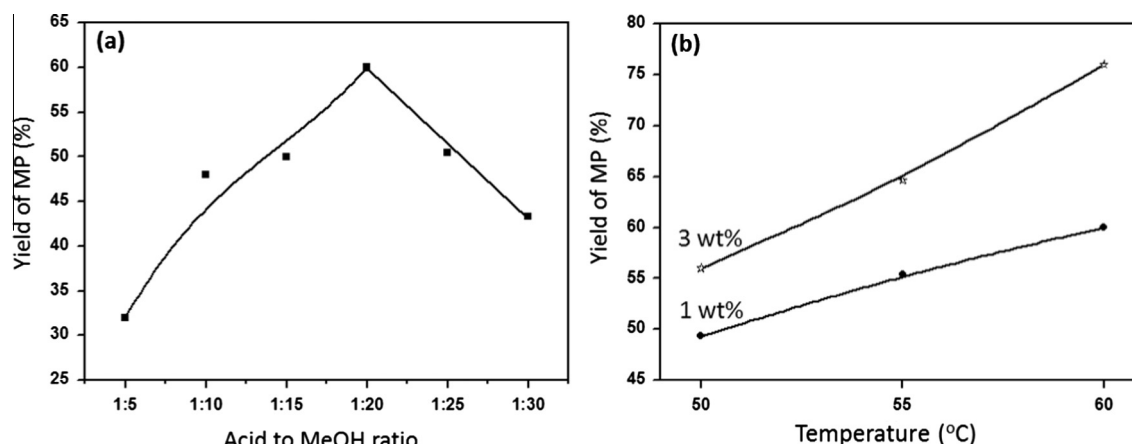


Fig. 3. Yield of methyl palmitate (MP) at varied (a) acid to methanol molar ratio and (b) temperature. Reaction conditions: Palmitic acid = 3 mmol and MeOH = 60 mmol; time = 7 h (a) temperature = 60 °C; catalyst = 1 wt%.

significantly lower than methyl palmitate (76%) at 60 °C due to the steric effect of increasing the alkyl chain of acid [39]. Thus, methanol is economical for the esterification of higher fatty acid owing to its lower boiling point that consumes lower thermal energy, producing higher yield of methyl esters and also it is cheaper than other alcohols.

3.2.4. Effect of catalyst concentration

The effect of catalyst amount showed that by increasing the catalyst amount from 1 to 5 wt%, the yield of methyl palmitate was linearly increased from 60% to 88%; and the yield was almost same (88–90%) by further increasing the catalyst amount to 6 wt% (Fig. 5). By increasing the catalyst amount, the number of acid sites increases, which favor the accessibility of more number of reactant molecules and thus resulted into increase in methyl palmitate yield. Therefore, further studies have been carried out over 6 wt% catalyst.

3.2.5. Effect of stirring speed

To study the effect of mass transfer, the catalytic experiments were conducted at different stirring speeds in the range of 500–800 rpm. The results showed slightly lower (85%) yield of methyl palmitate at 500 rpm, however, the yield was similar in the range of 89–91% at higher stirring speed of 600, 700 and 800 rpm (Fig. S4). These results indicated the absence of mass

transfer resistance at >600 rpm and the reactions were in kinetic regime. To ensure the pure kinetic regime all experiments were performed at a constant stirring speed of 700 rpm.

3.2.6. Kinetic studies

The kinetic profile of esterification reaction obtained with time in terms of the consumption of palmitic acid and formation of methyl palmitate is given in Fig. 7a. A sharp linear decrease in the concentration of palmitic acid was observed up to ~1 h; on further increasing the time decrease in concentration of acid became slow and started to approach saturation after 5 h. An identical trend in the formation of the methyl palmitate was also obtained.

The initial rates v , for the consumption of palmitic acid and v_1 , for the formation of methyl palmitate were calculated from the early linear portion of the graph (Fig. 6a) from the decreasing concentration of palmitic acid and increasing concentration of methyl palmitate, respectively by using the equations, $v = -d[PA]/dt$ and $v_1 = d[MP]/dt$. Under the optimized reaction conditions, both the rates v (0.66 mmol h⁻¹) and v_1 (0.61 mmol h⁻¹) were found to be almost equal indicating that there is a good balance between the concentration of the consumption of palmitic acid and selective formation of methyl palmitate. The kinetic investigations were performed by varying the amount of catalyst from 3 to 6 wt% by keeping other reaction conditions constant. The effect of variation

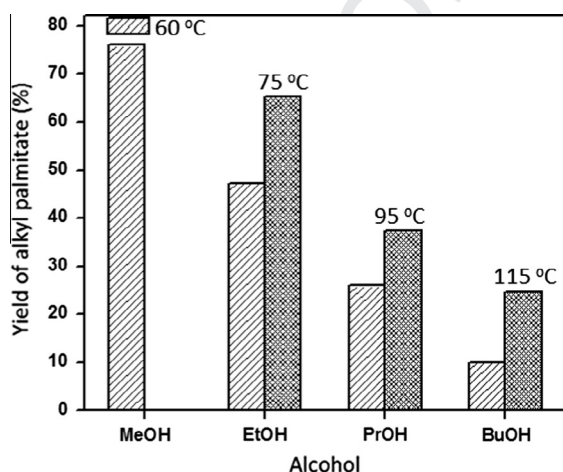


Fig. 4. Yield of various alkyl palmitate. Reaction conditions: Palmitic acid = 3 mmol and alcohol = 60 mmol; catalyst = 3 wt%; time = 7 h.

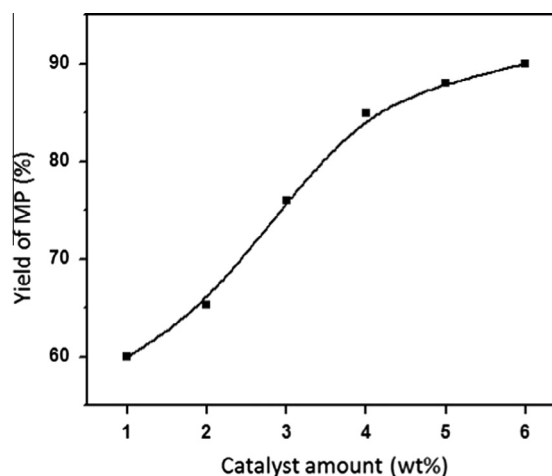


Fig. 5. Yield of methyl palmitate (MP) at varied catalyst amount. Reaction conditions: Palmitic acid = 3 mmol and MeOH = 60 mmol; temperature = 60 °C; time = 7 h.

in catalyst amount with respect to consumption of palmitic acid is given in Fig. 6b and the corresponding rates calculated from Fig. 6b are given in Fig. 7a.

The rate of formation of methyl palmitate was increased from 0.33 to 0.61 mmol h⁻¹ by increasing the catalyst amount (3–6 wt %) showing first order dependent of the catalyst amount. In order to observe the kinetic dependence of the substrates, the experiments carried out under typical conditions with 1:20 M ratio of palmitic acid and methanol gave a very good fitness of pseudo-first order kinetics in the plot of ln[PA] versus time (Fig. 7b). The pseudo-first order rate constant k (h⁻¹) calculated with different catalyst amount (3–6 wt%) were: $k \times 10^3$ (wt%) = 5.52 (3), 9.3 (4), 11.23 (5) and 12.13 (6). These rate constant were also increased in the line of the increasing of the rates on increasing the catalyst amount that further indicated first order dependence on the catalyst amount. The turnover frequency (TOF, mmoles of palmitic acid converted per mole of acid site concentration per min) was found to be 0.088 min⁻¹.

Though TOF of few reported solid acid catalysts like Cs-doped heteropolyacid (0.565 min⁻¹) [40] and sulfonated carbon (0.110 min⁻¹) [24] was high for the similar reaction, TOF of the SZr catalyst prepared in the present study was found to be higher (0.088 min⁻¹) as compared to reported SZr (0.031 min⁻¹) and SZr-SBA-15 (0.043 min⁻¹) catalysts [29] and also other catalysts such as sulfonated activated carbon (0.06 min⁻¹) [24], sulfonic acid-functionalized SBA-1 (0.04 min⁻¹) [41], sulfonated chitosan (0.009 min⁻¹) [18], poly(vinyl alcohol) cross-linked with sulfosuccinic acid (0.006 min⁻¹) [42], and 12-tungstophosphoric acid on niobia (0.0006 min⁻¹) [22].

In addition, the yield of methyl palmitate over SZr solid acid catalyst (90%) was found comparable with H₂SO₄ (95%) with an advantage of eco-friendly nature, ease of separation and re-use of solid acid catalyst.

3.2.7. Effect of solvent

The use of non-polar solvent such as hexane for the synthesis of biodiesel by transesterification of oils using homogeneous base catalyst has been reported to enhance the reaction rates by increasing the miscibility of oils in methanol [43]. Therefore, we have used hexane as a solvent; however, the results showed decreasing yield of methyl palmitate with a successive increase in hexane volume (Fig. 8). The yield was decreased to 71% at a solvent/reactants ratio of 1 (v/v) with respect to 84% under solvent free conditions. Though the solubility of palmitic acid is more in mixture of hexane with alcohols as compared to pure solvents [44], it displaces the palmitic acid from the active acid sites on the surface of the catalyst and thus lowers its interaction with

methanol resulting into decreased yield of methyl palmitate. Liu et al. [45] also found decrease in ester yield during the transesterification of poultry fat with methanol in presence of hydrotalcite solid base catalyst by using non-polar hexane, toluene as well as polar THF at a solvent/reactants ratio of 1 (v/v) due to the change in polarity that these co-solvents introduced to the reaction media. Therefore, all studies were done under solvent-free conditions.

4. Re-usability of the catalyst

The reusability of SZr catalyst was examined by carrying out successive reaction cycles. After completing the reaction, the catalyst was separated from the reaction mixture by centrifugation, washed by solvent to remove the adhered reactant and product molecules from the catalyst surface and thermally activated before next reaction with fresh reactants. The catalyst was washed by methanol: hexane mixture (~1:1) followed by activation at 600 °C temperature for 2 h under air flow. The results showed the decrease in the activity of used catalyst during each reaction cycle (Table 2). The re-sulfation of used catalyst between the reaction cycles was tried with an attempt to restore its activity and the yield of methyl palmitate was significantly increased to 81% compared to without re-sulfation (61%). The results indicated the need of re-sulfation of used catalyst for better reusability performance of the catalyst.

The possible reasons for the deactivation of the catalyst may be (i) loss of active sulfur sites (ii) coke deposition on the active sites. This was further confirmed by the characterization of re-used catalyst after five reaction cycles. The FT-IR spectrum (Fig. S5) of re-used (SZr-ru) catalyst (washed with methanol: hexane and oven dried at 120 °C, 12 h) showed peaks at 1537, 1459, 1407, 2918, 2850 cm⁻¹ which are assigned to the bending/scissoring and stretching vibration of C–H, –CH₂–/–CH₃ groups. The spectrum provides evidence of the strong adsorption of bulky palmitic acid/ester product molecules on the catalyst surface which was not completely washed out by simple solvent washing. The FT-IR spectrum of activated (SZr-ac) catalyst (re-calcination at 600 °C for 2 h in air flow) showed the absence of these peaks indicating the removal of organic moieties from the surface of the catalyst (Fig. S5). The elemental analysis showed 1.76 wt% carbon in re-used, SZr-ru catalyst, which was significantly decreased after activation in SZr-ac catalyst (0.02 wt%). It is reported that a small amount of coke deposition, e.g., only 0.06 wt% may result in complete deactivation of SZr for *n*-butane isomerization [46].

However, the sulfur content of the used catalyst was found to decrease continuously after each reaction cycle and was 0.60 wt%

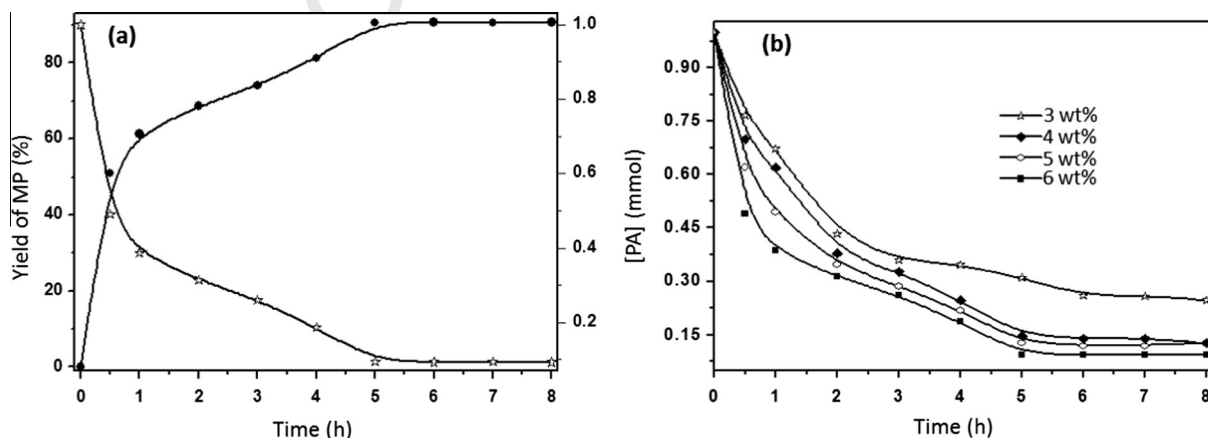


Fig. 6. Reaction profile for esterification of palmitic acid (PA) with time over (a) 6 wt% and (b) varied catalyst amount. Reaction conditions: PA = 3 mmol and MeOH = 60 mmol; temperature = 60 °C.

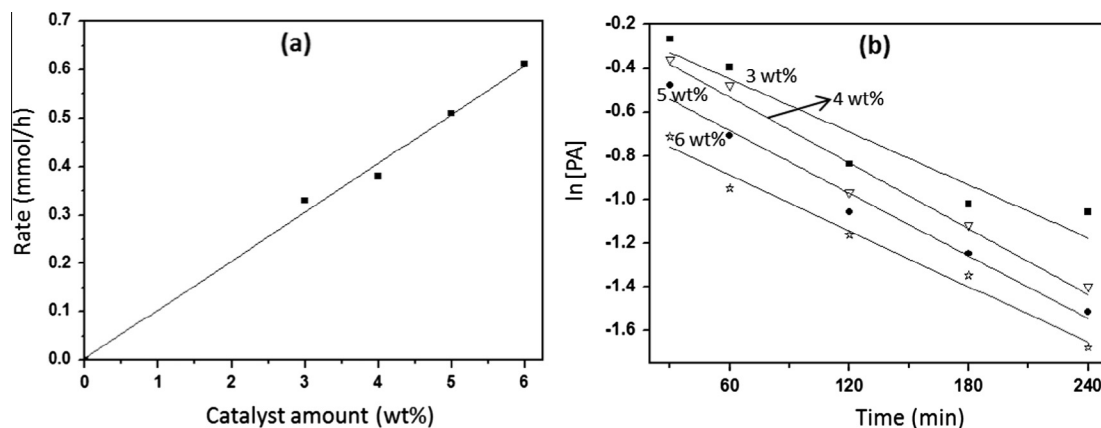


Fig. 7. (a) Rate of esterification of palmitic acid (PA) with methanol for varied catalyst amount and (b) plot of ln [PA] versus time.

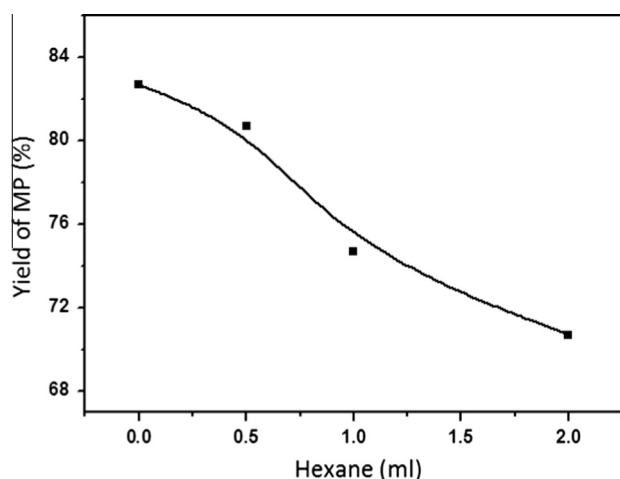


Fig. 8. Effect of hexane-solvent on esterification of palmitic acid (PA) with methanol. Reaction conditions: PA = 3 mmol and MeOH = 60 mmol; catalyst = 6 wt %; time = 4 h; temperature = 60 °C.

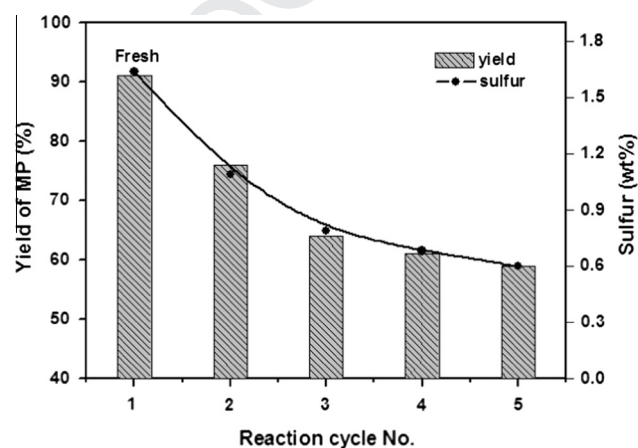


Fig. 9. Co-relation of decreased yield of methyl palmitate with sulfur content after each reaction cycle.

after five reaction cycles (Table 2) indicating the loss of sulfur during the reaction. The yield of methyl palmitate was decreased accordingly (Fig. 9). As acidity of SZr catalyst depends on the amount of sulfur, B/L ratio of the final SZr (SZr-ac) catalyst was calculated and was found to decrease from 1.48 (fresh) to 1.00 (after 5th cycle) suggesting the loss of few active acid sites. DRIFT spectra of SZr-ac catalyst showed the presence of both Brönsted and Lewis acid sites present till 450 °C (Fig. S6), however, the intensity of the peaks were lower as compared to fresh catalyst (Fig. S3).

To check the possibility of lost/leached sulfur during the reaction, we have characterized the ester product of subsequent five reaction cycles by FT-IR and elemental analysis. The FT-IR spectra (Fig. S7) showed the intense peaks at 1743, 1174 and 1464 cm⁻¹,

which were assigned to C=O, C–O stretching and C–H bending respectively along with 2920 and 2855 cm⁻¹ for C–H stretching in methyl palmitate product [47]. The appearance of small peak at 1701 cm⁻¹ for C=O stretching (acid) with intense peak of C=O (ester at 1743 cm⁻¹) in product showed the presence of unreacted acid as conversion of acid decreased with successive reaction cycles. FT-IR spectrum of one of the reaction mixture having methanol (after 3rd cycle) also showed these peaks along with an intense peak at 1030 cm⁻¹ and a broad peak at 3390 cm⁻¹, which were assigned to O–H and C–O stretching of methanol [48]. There is a probability of the formation of sulfur complex with methyl ester product, however it was difficult to identify any new peak assignable for sulfur/sulfur complex due to the resemblance of several peaks in the product in the region of 1200–942 cm⁻¹ with sulfate region. The sulfur was also not detectable in the elemental analysis of the ester product after each reaction cycle.

Table 2

Yield of methyl palmitate over fresh and re-used SZr catalyst.

Reaction cycle no.	Yield of methyl palmitate (%) ^a
1 (Fresh)	91
2	76
3	64
4	61 (81 ^b)
5	59

^a Reaction conditions: Acid:MeOH molar ratio = 1:20; catalyst = 6 wt%; time = 5 h; temperature = 60 °C.

^b Catalyst was re-sulfated.

5. Conclusions

Sulfated zirconia catalyst, prepared by simple conventional precipitation method, exhibited an excellent activity for the esterification of palmitic acid with methanol having 90% yield of methyl palmitate at 60 °C after 5–7 h over 6 wt% catalyst amount. The yield of corresponding esters with increasing carbon chain of alcohols namely ethanol, *n*-propanol and *n*-butanol was decreased at 60 °C and moderately increased by increasing the reaction temperature near to the boiling point of the respective alcohols.

The studied reaction follows pseudo-first order kinetics under the employed reaction conditions with a reaction rate of 0.61 mmol h^{-1} , rate constant of $12.13 \times 10^{-3} \text{ h}^{-1}$ and turn over frequency of 0.088 min^{-1} over 6 wt% catalyst. The yield of methyl palmitate was significantly higher under solvent-free conditions as compared to when hexane was used as a solvent. The decreased activity of the catalyst was attributing to sulfur loss, however, it was not in detectable limits. The activity of re-used catalyst was enhanced by re-sulfation.

Acknowledgements

CSIR-CSMCRI Communication No. 225/2014. Authors are thankful to CSIR Network Programme on Clean Coal Technology (TabCoal CSC-102) for financial assistance and to 'Analytical Discipline and Centralized Instrumental Facilities' for providing instrumentation facilities.

Appendix A. Supplementary material

Supplementary data associated with this article can be found, in the online version, at <http://dx.doi.org/10.1016/j.fuel.2015.10.043>.

References

- [1] Lee D-W, Lee K-Y. Heterogeneous solid acid catalysts for esterification of free fatty acids. *Catal Surv Asia* 2014;18:55–74.
- [2] Furuta S, Matsuhashi H, Arata K. Biodiesel fuel production with solid superacid catalysis in fixed bed reactor under atmospheric pressure. *Catal Commun* 2004;5:721–3.
- [3] Corro G, Bañuelos F, Vidal E, Cebada S. Measurements of surface acidity of solid catalysts for free fatty acids esterification in *Jatropha curcas* crude oil for biodiesel production. *Fuel* 2014;115:625–8.
- [4] Supple B, Holward-Hildige R, Gonzalez-Gomez E, Leahy JJ. The effect of steam treating waste cooking oil on the yield of methyl ester. *J Am Oil Chem Soc* 2002;79(2):175–8.
- [5] Cvangros J, Cvangrosova Z. Used frying oils and fats and their utilization in the production of methyl esters of higher fatty acids. *Biomass Bioenergy* 2004;27:173–81.
- [6] Ki-Teak L, Foglia TA, Chang K. Production of alkyl ester as biodiesel from fractionated lard and restaurant grease. *J Am Oil Chem Soc* 2002;79(2):191–5.
- [7] Sani YM, Daud WMAW, Abdul Aziz AR. Activity of solid acid catalysts for biodiesel production: a critical review. *Appl Catal A* 2014;470:140–61.
- [8] Crabbe E, Nolasco-Hipolito C, Kobayashi G, Sonomoto K, Ishizaki A. Biodiesel production from crude palm oil and evaluation of butanol extraction and fuel properties. *Process Biochem* 2001;37:65–71.
- [9] <http://www.sigmaaldrich.com/catalog/product/aldrich/w509531?lang=en®ion=IN>.
- [10] Freedman B, Pryde EH, Mounts TL. Variables affecting the yields of fatty esters from transesterified vegetable oils. *J Am Oil Chem Soc* 1984;61:1638–43.
- [11] Zheng S, Kates M, Dubé MA, McLean DD. Acid-catalyzed production of biodiesel from waste frying oil. *Biomass Bioenergy* 2006;30:267–72.
- [12] Jacobson K, Gopinath R, Meher LC, Dalai AK. Solid acid catalyzed biodiesel production from waste cooking oil. *Appl Catal B* 2008;85:86–91.
- [13] Lotero E, Liu Y, Lopez DE, Suwannakarn K, Bruce DA, Goodwin Jr JG. Synthesis of biodiesel via acid catalysis. *Ind Eng Chem Res* 2005;44:5353–63.
- [14] Sharma YC, Singh B, Korstad J. Advancements in solid acid catalysts for ecofriendly and economically viable synthesis of biodiesel. *Biofuels Bioprod Bioref* 2011;5:69–92.
- [15] Melero JA, Iglesias J, Morales G. Heterogeneous acid catalysts for biodiesel production: current status and future challenges. *Green Chem* 2009;11:1285–308.
- [16] Ramu S, Lingaiah N, Prabhavathi Devi BLA, Prasad RBN, Suryanarayana I, Prasad PSS. Esterification of palmitic acid with methanol over tungsten oxide supported on zirconia solid acid catalysts: effect of method of preparation of the catalyst on its structural stability and reactivity. *Appl Catal A* 2004;276:163–8.
- [17] Rao KN, Sridhar A, Lee AF, Tavener SJ, Young NA, Wilson K. Zirconium phosphate supported tungsten oxide solid acid catalysts for the esterification of palmitic acid. *Green Chem* 2006;8:790–7.
- [18] Caetano CS, Caiado M, Farinha J, Fonseca IM, Ramos AM, Vital J, et al. Esterification of free fatty acids over chitosan with sulfonic acid groups. *Chem Eng J* 2013;230:567–72.
- [19] Tropeçelo AI, Casimiro MH, Fonseca IM, Ramos AM, Vital J, Castanheiro JE. Esterification of free fatty acids to biodiesel over heteropolyacids immobilized on mesoporous silica. *Appl Catal A* 2010;390:183–9.
- [20] Brahmkhatri V, Patel A. Biodiesel production by esterification of free fatty acids over 12-tungstophosphoric acid anchored to MCM-41. *Ind Eng Chem Res* 2011;50:6620–8.
- [21] Caetano CS, Fonseca IM, Ramos AM, Vital J, Castanheiro JE. Esterification of free fatty acids with methanol using heteropolyacids immobilized on silica. *Catal Commun* 2008;9:1996–9.
- [22] Srilatha K, Lingaiah N, Devi BLAP, Prasad RBN, Venkateswar S, Prasad PSS. Esterification of free fatty acids for biodiesel production over heteropoly tungstate supported on niobia catalysts. *Appl Catal A* 2009;365:28–33.
- [23] Giri BY, Rao KN, Devi BLAP, Lingaiah N, Suryanarayana I, Prasad RBN, et al. Esterification of palmitic acid on the ammonium salt of 12-tungstophosphoric acid: the influence of partial proton exchange on the activity of the catalyst. *Catal Commun* 2005;6:788–92.
- [24] Poonjarernsilp C, Sano N, Tamon H. Hydrothermally sulfonated single-walled carbon nanohorns for use as solid catalysts in biodiesel production by esterification of palmitic acid. *Appl Catal B* 2014;147:726–32.
- [25] Carmo AC, de Souza LKC, da Costa CEF, Longo E, Zamian JR, da Rocha Filho GN. Production of biodiesel by esterification of palmitic acid over mesoporous aluminosilicate Al-MCM-41. *Fuel* 2009;88:461–8.
- [26] Baig A, Ng Flora TT. A single-step solid acid-catalyzed process for the production of biodiesel from high free fatty acid feedstocks. *Energy Fuels* 2010;24:4712–20.
- [27] Chen G, Guo C-Y, Qiao H, Ye M, Qiu X, Yue C. Well-dispersed sulfated zirconia nanoparticles as high-efficiency catalysts for the synthesis of bis(indolyl) methanes and biodiesel. *Catal Commun* 2013;41:70–4.
- [28] Su F, Guo Y. Advancements in solid acid catalysts for biodiesel production. *Green Chem* 2014;16:2934.
- [29] Chen X-R, Ju Y-H, Mou C-Y. Direct synthesis of mesoporous sulfated silica-zirconia catalysts with high catalytic activity for biodiesel via esterification. *J Phys Chem C* 2007;111:18731–7.
- [30] (a) Saravanan K, Tyagi B, Bajaj HC. Catalytic activity of sulfated zirconia solid acid catalyst for esterification of myristic acid with methanol. *Ind J Chem* 2014;53A:799; (b) Saravanan K, Tyagi B, Bajaj HC. Sulfated zirconia: an efficient solid acid catalyst for esterification of myristic acid with short chain alcohols. *Catal Sci Technol* 2012;2:2512–20.
- [31] Cullity BD, Stock SR. Elements of X-ray diffraction. 3rd ed. Upper Saddle River: Prentice Hall; 2001. p. 388.
- [32] Tyagi B, Chudasama CD, Jasra RV. Characterization of surface acidity of an acid montmorillonite activated with hydrothermal, ultrasonic and microwave techniques. *Appl Clay Sci* 2006;31:16–28.
- [33] Emeis CA. Determination of integrated molar extinction coefficients for infrared absorption bands of pyridine adsorbed on solid acid catalysts. *J Catal* 1993;141:347–54.
- [34] Barzetti T, Selli E, Moschetti D, Forni L. Pyridine and ammonia as probes for FTIR analysis of solid acid catalysts. *J Chem Soc, Faraday Trans* 1996;92:1401–7.
- [35] Satyarthi JK, Radhakrishnan S, Srinivas D. Factors influencing the kinetics of esterification of fatty acids over solid acid catalysts. *Energy Fuels* 2011;25:4106–12.
- [36] Yamaguchi T, Jin T, Tanabe K. Structure of acid sites on sulfur-promoted iron oxide. *J Phys Chem* 1986;90:3148–52.
- [37] Gregg SJ, Sing KSW. Adsorption, surface area and porosity. 2nd ed. New York: Academic Press; 1982.
- [38] Armendariz H, Cortes MA, Hernandez I, Navarrete J, Vazquez A. One-step synthesis and characterization of $\text{ZrO}_2\text{-WO}_x$ prepared by hydrothermal method at autogenous pressure. *J Mater Chem* 2003;13:143–9.
- [39] Liu Y, Lotero E, Goodwin Jr JG. Effect of carbon chain length on esterification of carboxylic acids with methanol using acid catalysis. *J Catal* 2006;243:221–8.
- [40] Narasimharao K, Brown DR, Lee AF, Newman AD, Siril PF, Tavener SJ, et al. Structure-activity relations in Cs-doped heteropolyacid catalysts for biodiesel production. *J Catal* 2007;248:226–34.
- [41] Abbasi A, Mahjoub AR, Badiei AR. A novel highly acidic sulfonic functionalized SBA-1 cubic mesoporous catalyst and its application in the esterification of palmitic acid. *Mater Sci-Poland* 2010;28:565–72.
- [42] Caetano CS, Guerreiro L, Fonseca IM, Ramos AM, Vital J, Castanheiro JE. Esterification of fatty acids to biodiesel over polymers with sulfonic acid groups. *Appl Catal A* 2009;359:41–6.
- [43] Peña R, Romero R, Martínez SL, Ramos MJ, Martínez A, Natividad R. Transesterification of castor oil: effect of catalyst and co-solvent. *Ind Eng Chem Res* 2009;48:1186–9.
- [44] Calvo B, Collado I, Cepeda EA. Solubilities of palmitic acid in pure solvents and its mixtures. *J Chem Eng Data* 2009;54:64–8.
- [45] Liu Y, Lotero E, Goodwin Jr JG, Mo X. Transesterification of poultry fat with methanol using Mg–Al hydrotalcite derived catalysts. *Appl Catal A* 2007;331:138–48.
- [46] Li B, Gonzalez RD. An in situ DRIFTS study of the deactivation and regeneration of sulfated zirconia. *Catal Today* 1998;46:55–67.
- [47] http://www.chemicalbook.com/SpectrumEN_112-39-0_IR1.htm.
- [48] Falk M, Whalley E. Infrared spectra of methanol and deuterated methanols in gas, liquid, and solid phases. *J Chem Phys* 1961;34:1554–68.